

Segmentation of the LV and RV endocardium and epicardium

Abdullah Thabit
Roa'a Khaled
Medical Sensors - MAIA
University of Burgundy

January 6, 2019

Abstract

Segmentation of the heart ventricles have been an important clinical tool that cardiologists use to diagnose cardiac diseases. In this work, basic but powerful image processing techniques has been leveraged to drive an intensity-based image segmentation for the Left Ventricle (LV) endocardium and epicardium as well as the Right Ventricle (RV). A Region of Interest (ROI) was detected automatically at first, then the LV and RV endocardial countours were segmented with respect to a marker. Finally the epicardium was delineated by taking advantage of transformring the ROI to the polar coordinates. The results obtained were good in detecting the three contours, but were also highly dependent on the image contrast, leading to changes in accuracy from patient to patient.

1 Introduction

Segmentation of the LV and RV is an important clinical tool since it is a prerequisite to compute the cardiac parameters for patients in order to help cardiologists to diagnose myocardial diseases. The manual segmentation process has many disadvantages. It is subjective and time consuming. Thus, many different automated methods have been suggested. We have chosen to implement pixel based classification methods because of the advantages of such methods over the other methods. According to [1] methods that rely primarily on image information are less computationally demanding and does not require any complex shape or gray level appearance models which has to be constructed from many manually segmented images. The methods we have chosen to implement use simple prior knowledge about the heart and the used MRI images. Also they are not restricted only to the LV endocardial segmentation, but also they segment the RV and the epicardium. For this segmentation task, we implemented methods suggested in three different articles which are primarily image driven methods. Our segmentation tool was developed at three stages. The first is the selection of ROI for which we have implemented the method suggested by [1]. The second

is the segmentation of the LV and RV endocardium, for which we have implemented the method suggested by [2]. And the last is the segmentation of the LV epicardium, for which we have implemented the method suggested by [3].

In the following section, we are describing the method implemented for each stage of the whole segmentation task.

2 Method

2.1 Selection of the ROI

Restricting the image into a region of interest is an important first step to be done before the segmentation. This comes from the fact that the field of view (FOV) of the short axis MRI slices is larger than the heart (which may not be exactly in the centre of the FOV), so if the segmentation process will be done on the whole FOV of the image it will take longer computational time and false objects might be detected as a heart. Thus, most methods starts with obtaining a restrictive ROI within the images which will reduce the computational time of the segmentation process and increase the segmentation accuracy.

To select the ROI we have implemented the method suggested in [1] which is fully automatic. It is based on the following assumptions:

- 1- The intensities of the voxels at the myocardium boundaries are extremely varying along the cardiac cycle within the 3D + time MRI cardiac images.
- 2- The long axis of the heart roughly corresponds to the z axis of the 3D image. However this assumption is limited to a properly acquired short axis scan.
- 3- The shape of the heart in short axis images has a convex shape if we ignore the small irregularities due to the pappillary muscles or heart wall abnormalities.
- 4- If we apply a maximum intensity projection along the z axis of the 3D image, the resulted largest spatial grouping of voxels will correspond to the heart because they represent the voxels of the highest temporal variability of the intensity along the time dimension.

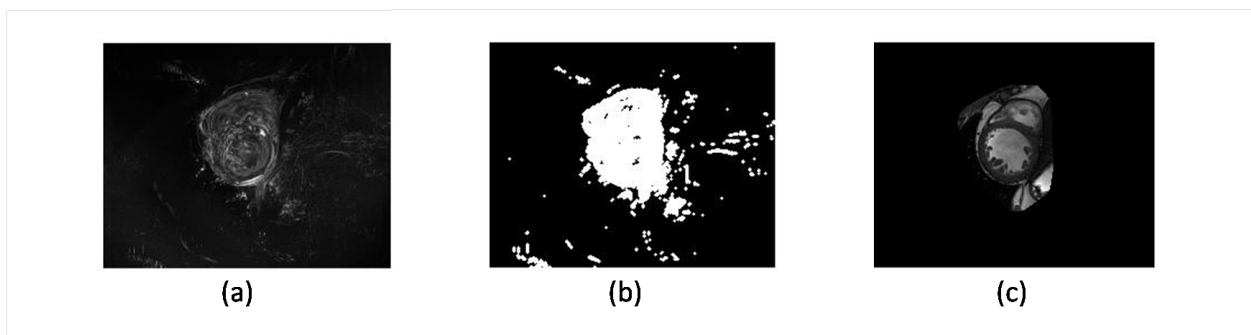
The method of ROI extraction was implemented by applying the following steps. The first step of selecting the ROI was to compute the standard deviation of the 3D+time image intensity along the time dimension, this is to detect the voxels of high temporal change in their intensities. The result of this step is a 3D image. The second step is applying a maximum intensity projection along the z dimension of the 3D image obtained from the first step, this will result in a 2D image as shown in figure (1-a). The third step is to smooth the 2D image obtained from step 2 using Gaussian filter with a 2-D Gaussian smoothing kernel and standard deviation of 0.5 (which has been chosen empirically). The goal of this step is to eliminate the small features and reduce the artifacts.

The forth step is to threshold the smoothed 2D using Otsu method. Other thresholding methods could be used, however this method is automatic and does not require any parameters to be selected. The fifth step is to apply the dilation morphological operation (8 times, which was also chosen empirically). The next step was to find the binary connected com-

ponents using 2D four connected neighborhood. Figure (1-b) shows the dilated thresholded image. The largest connected components were obtained by taking those with the largest number of pixels (i.e. removing the small objects).

Finally, a 2D convex hull of the binary image is computed by the assumption that the heart has a convex shape in short axis MRI slices. This step is important for increasing the robustness especially for cases with abnormal myocardium due to reduced contraction (as the case in some cardiac diseases). The final output is a 2D ROI which can be extended to the whole 3D+time image by imposing it to all slices in all time frames. Figure (1-c) shows the Final ROI on a sample slice.

Figure 1: (a) Output image after applying MI. to the standard deviation of the 3D image along the time dimension (b) The output after thresholding and dialation. (c) The final ROI of a sample slice.



2.2 LV and RV endocardium segmentation

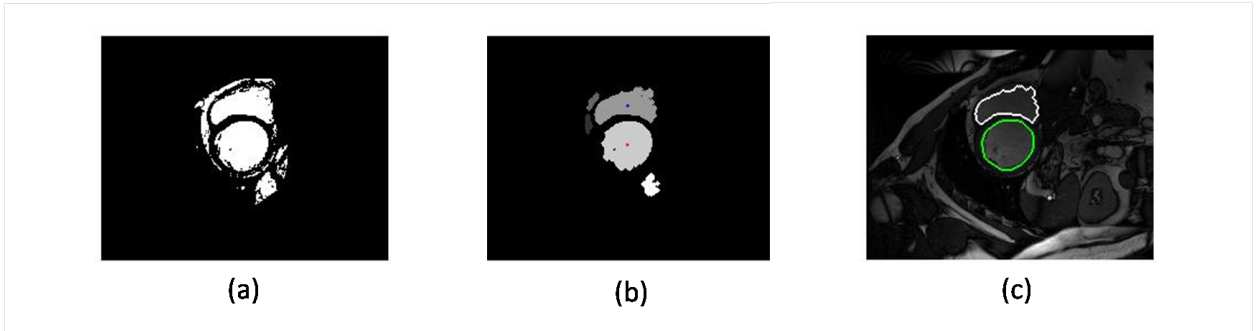
After obtaining the ROI we applied the method presented in [2] for segmenting the LV and RV endocardium. The first step is to select the LV cavity by asking the user to select a point (marker) inside the LV cavity. The second step is to apply the power law transformation to the ROI image. This step enhances the myocardium contrast and helps differentiating between it and the cavity. We used the same values of the power law parameters selected by the authors ($k=1$, $=1.3$). The third step is to threshold the transformed image using Otsu method. Figure (2-a) shows the output of thresholding. The fourth step is to remove the small objects by applying morphological operations (dilation and erosion). We applied dilation twice and then erosion twice using 2D four connected neighborhood. The next step is to obtain the connected components and keeping only the 5 largest ones, by taking the components with the largest number of pixels. After this, the largest objects kept from previous step are labeled and their centroids are calculated.

To locate the LV cavity, the distances between those largest objects' centroids and the point selected at the beginning (marker) were computed. The minimum distance then is obtained which corresponds to the distance between the LV cavity and the marker, hence the LV cavity is located. The next step is to locate the RV. Since the RV is the nearest object to

the LV cavity, the distances between each object's centroid and the LV cavity centroid are calculated and the minimum of those distances is found, which leads to locating the RV. Figure (2-b) shows the LV and RV labeled with their centroids marked.

One last step is performed in order to remove the irregularities in the borders of both RV and LV endocardium. For the RV, the holes are filled and the border is smoothed. For the LV, the convex hull was computed to exclude the papillary muscles. Figure (2-c) shows the final output with the LV and RV segmented.

Figure 2: (a) sample slice image after thresholding. (b) The largest 5 objects labeled with the LV and RV centroids marked. (c) Segmented LV and RV contours.



2.3 LV epicardium segmentation

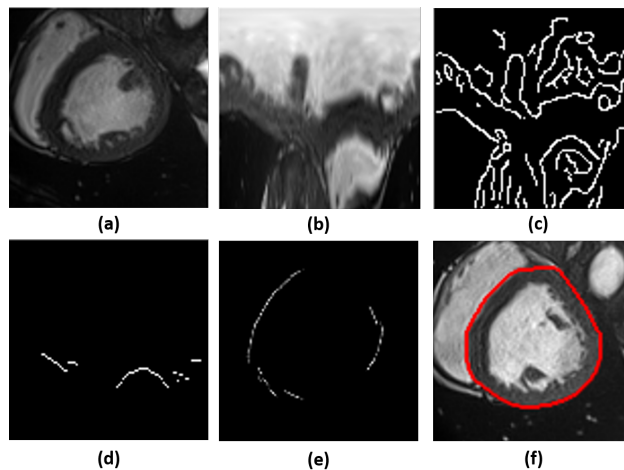
Epicardial contour segmentation is known to be a more difficult task than it is for the endocardial contours. Inhomogeneity, presence of fatty tissues, and the surrounding tissues of the myocardium all contribute to this arising difficulty.

Therefore, for segmenting the epicardial contour, a sub-image (square window) of 100 pixels in width and height, and centered on the LV centroid was extracted. Another window of the same size was also extracted for the LV binary image to be used as a mask. The LV mask was dilated with an 8-connectivity structuring element to make sure it fully covers the LV cavity. Then both, gray level sub-image and the mask were converted from the cartesian coordinates to the polar coordinates [4]. It is known that circular contours in the cartesian coordinates appear as lines in the polar coordinates, making it easier to segment the epicardium, as shown in Figure (3).

Canny edge detection was then applied to the gray level sub-image, resulting in two horizontal lines and many other small connected components. These two lines refer to the endocardial and epicardial contours of the LV. To eliminate the endocardial contour and any connected components inside the cavity, a complement of the mask was applied to the edged binary sub-image. Also, since we are interested only in the epicardium horizontal line, morphological opening with a rectangular structuring element was applied to reduce and eliminate vertical connected components. Then, the epicardial horizontal edge was detected by keeping the first point (white pixel) in each column of the sub-image, and setting to zero all other pixels.

The remaining outliers are then eliminated by finding the average location of the edge line and setting to zeros all pixels outside a margin of 10 pixels, keeping only the pixels that contribute to the epicardial edge line. Finally, the sub-image of the epicardium edge is then converted back to the cartesian coordinates and further processed by eliminating connected components that are less than 5 pixels before finding the convex hull of the epicardium and delineate its contour. See the steps in Figure (3) below.

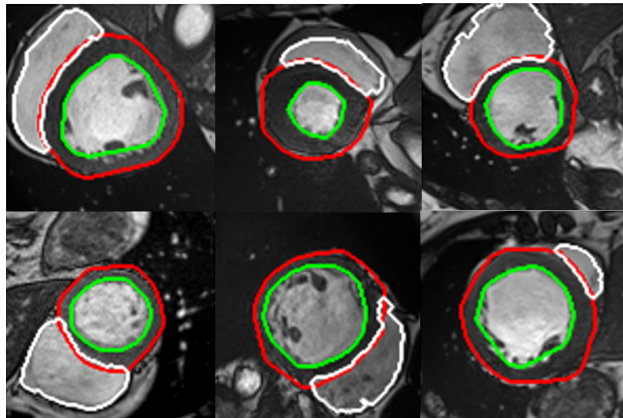
Figure 3: Epicardium segmentation: (a) gray level subimage window (b) subimage window in the polar coordinates, (c) canny edges of the polar subimage,(d) epicardium edge line (e) epicardium contour in the cartesian coordinates , (f) epicardium contour



3 Results And Discussion

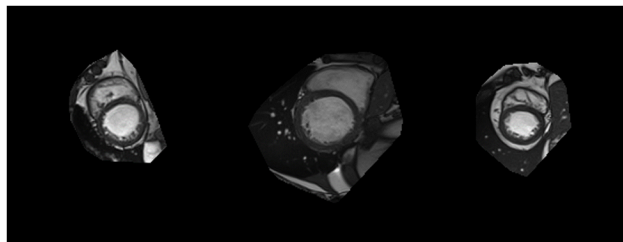
In this project, we have leveraged basic image processing techniques to segment both LV and RV cavities as well as the LV epicardium. Our algorithm was tested on the 100-patients training dataset provided in the MICCAI challenge 2017 [5]. The algorithm was tested by overlaying the segmented contours on the gray level images and assessing the accuracy visually. MATLAB 2017b was used for programming and the Tools for Nifti images [6] were used to read the Nifti data. Given the simplicity and speed of the algorithm, it performed well in segmenting both LV endocardial and epicardial contours and also the RV in many patients, especially around the mid slice and when the image contrast is good. Figure (4) shows samples of the segmented contours.

Figure 4: algorithm segmentation results for the LV endocardial (green), RV endocardial (white) and LV epicardial contour (red)



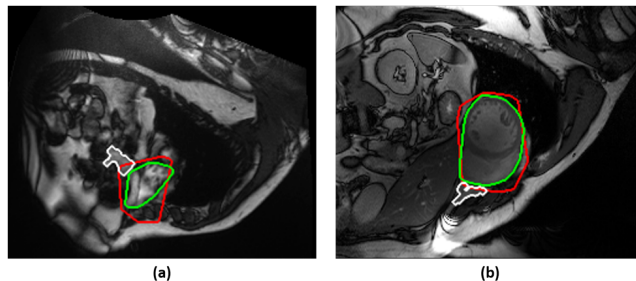
For the ROI method, the algorithm was capable to locate the patients heart almost all the time in all short-axis images with only one exception, where it failed in detecting the ROI for patient number 73 in the dataset. Figure (5) below shows some of the results for the ROI detection.

Figure 5: sample results of the ROI detection



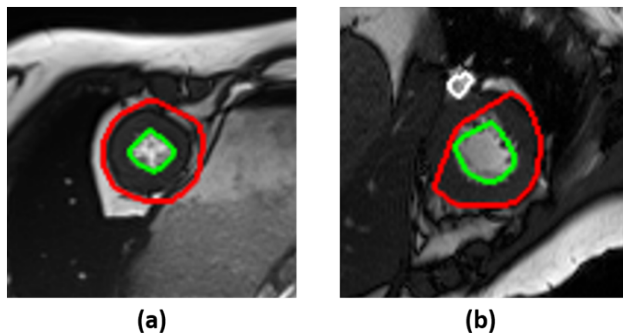
The algorithm showed good accuracy in segmenting the LV cavity, with only very few major failures (mainly on the first or last slice at the apex). However, one could argue that even manual tracing of the LV endocardial contours the gold standard for these images is very difficult, as shown in Figure (6-a). Another major failure in segmenting the LV endocardial resulted from the poor image contrast for some patients images, where the RV cavity was mistakenly considered as part of the LV cavity as shown in Figure (6-b) below, which is one of the main disadvantages of intensity-based image segmentation methods that they are highly dependent on the image quality and lighting conditions.

Figure 6: LV endocardial segmentation failed; (a) LV cavity is not clear in the image, (b) myocardium contrast is very low and the RV is detected as part of the LV



The accuracy of the RV endocardial segmentation was the least among the three segmented contours, and that came mainly due to the shape-irregularity of the RV, which also make it hard to segment manually for not well-trained eyes. In our algorithm, major failure in segmenting the RV appeared to happen either because another detected tissue was closer to the LV and therefore was segmented as the RV, or because it was small and got eliminated with other small connected components. Although the Epicardium is usually harder to detect with intensity-based image segmentation techniques due to the reasons discussed above, our algorithm gave good results for many patients in slices that are around the mid slice; whereas in some slices near both atria and apex, epicardial contour was either larger than the actual contour or it cuts through the myocardium, as shown in Figure (7).

Figure 7: samples of epicardium segmentation errors; (a) epicardium contour is larger than the actual one, (b) epicardial contour cuts through the myocardium



4 Conclusion

The algorithm developed here tends to perform well in controlled conditions, where the contrast is very good; however, that is usually not the case in clinical settings. This algorithm appeared to be rigid and cannot accommodate for the inter-changes between patients if high accuracy segmentation is the goal; therefore, it cannot be used as a stand-alone technique for ventricles segmentation, but rather it can serve as a preprocessing step for more advanced algorithms, especially the ROI method discussed earlier. A couple of improvements can be conducted to further enhance this technique, such as, taking advantages of the shape-prior

information (circularity) of the LV to eliminate the need for the marker and make the algorithm fully automatic. Also, the algorithm accuracy can be further assessed quantitatively by calculating the dice and compare it with a manually traced reference and other state of the art techniques.

5 References

- [1] C. Cocosco, W. Niessen, T. Netsch, E. Vonken, G. Lund, A. Stork, and M. Viergever, "Automatic Image-Driven Segmentation of the Ventricles in Cardiac Cine MRI", JOURNAL OF MAGNETIC RESONANCE IMAGING 28:366374 (2008)
- [2] A. Katouzian, A. Prakash and E. Konofagou1, "A NEW AUTOMATED TECHNIQUE FOR LEFT- AND RIGHT-VENTRICULAR SEGMENTATION IN MAGNETIC RESONANCE IMAGING", Proceedings of the 28th IEEE, EMBS Annual International Conference, New York City, USA, Aug 30-Sept 3, 2006
- [3] M. Hadhoud, M. Eladawy, A. Farag, F. Monteverchi, U. Morbiducci, "Left Ventricle Segmentation in Cardiac MRI Images", American Journal of Biomedical Engineering 2012, 2(3): 131-135
- [4] P. Manandhar Polar To/From Rectangular Transform of Images, V0.1 16 Dec 2007, <https://www.mathworks.com/matlabcentral/fileexchange/17933-polar-to-from-rectangular-transform-of-images>
- [5] O. Bernard, A. Lalande, C. Zotti, F. Cervenansky, et al. "Deep Learning Techniques for Automatic MRICardiac Multi-structures Segmentation andDiagnosis: Is the Problem Solved?" in IEEE Transactions onMedical Imaging,vol. 37, no. 11, pp. 2514-2525, Nov. 2018
- [6] J. Shen, Tools for NIFTI and ANALYZE image, version 1.27.0.0, <https://www.mathworks.com/matlabcentral/fileexchange/17933-polar-to-from-rectangular-transform-of-images>